International Journal of Bifurcation and Chaos, Vol. 18, No. 5 (2008) 1567–1577
© World Scientific Publishing Company

A MINIMAL 2-D QUADRATIC MAP WITH QUASI-PERIODIC ROUTE TO CHAOS

ZERAOULIA ELHADJ
Department of Mathematics, University of Tébéssa, (12000), Algeria
zeraoulia@mail.univ-tebessa.dz
zelhadj12@yahoo.fr

J. C. SPROTT
Department of Physics, University of Wisconsin, Madison, WI 53706, USA
sprott@physics.wisc.edu

Received April 19, 2007; Revised May 30, 2007

The aim of this paper is to present and analyze a minimal chaotic map of the plane, then we describe in detail the dynamical behavior of this map, along with some other dynamical phenomena.

Keywords: Minimal 2-D quadratic chaotic map; quasi-periodic route to chaos.

1. Introduction

The Hénon map [Hénon, 1976] given by

$$h(x,y) = \begin{pmatrix} 1 - ax^2 + by \\ x \end{pmatrix} \tag{1}$$

has been widely studied because it is the simplest example of a dissipative map with chaotic solutions. It has a single quadratic nonlinearity and an area contraction that depends only on b and is thus constant over the orbit in the xy-plane. It can also be written as a one-dimensional time-delayed map:

$$x_{n+1} = 1 - ax_n^2 + bx_{n-1}. \tag{2}$$

Generalizations of this map [Benedicks & Carleson, 1991; Aziz-Alaoui *et al.*, 2001] have contributed to the development of dynamical systems theory and have produced new chaotic attractors with applications in science and engineering [Newcomb & Sathyan, 1983; Grassi & Mascolo, 1999]. Application areas include secure communication and information processing [Newcomb & Sathyan, 1983; Grassi & Mascolo, 1999] where discrete-component electronic implementation is possible [Andreyev & Belsky, 1996].

Here we propose and analyze an equally simple two-dimensional quadratic map given by

$$f(x,y) = \begin{pmatrix} 1 - ay^2 + bx \\ x \end{pmatrix}, \tag{3}$$

where a and b are bifurcation parameters. Equation (3) is an interesting minimal system, similar to the Hénon map, but with the time delay in the nonlinear rather than the linear term as evidenced by writing it in the time-delayed form:

$$x_{n+1} = 1 - ax_{n-1}^2 + bx_n. \tag{4}$$

Despite its apparent similarity and simplicity, it differs from the Hénon map in that it has a nonuniform dissipation, a more rich and varied route to chaos, and a much wider variety of attractors. Whereas the attractors for the Hénon map have a maximum dimension of about 1.31, with all the attractors qualitatively similar, the map (3) has attractors covering the entire range of dimensions from 1 to 2

(as well as zero) with basins of attraction that are often much more complicated than for the Hénon map. These systems are special cases of general 2-D quadratic maps, many examples of which are given by Sprott [1993] but not extensively studied.

Equation (4) reduces to the time-delayed quadratic map for $b = 0$, much as the Hénon map in Eq. (2) reduces to the ordinary quadratic map for $b = 0$. On the other hand, this system is different from other well-known 2-D maps such as the delayed logistic map [Aronson & Chory, 1982] given by

$$g(x, y) = \begin{pmatrix} ax(1-y) \\ x \end{pmatrix}. \tag{5}$$

Equation (3) is not topologically equivalent to Eq. (5) since the latter has two fixed points $(0, 0)$ and $((a-1)/a, (a-1)/a)$ that exist for all values of $a \neq 0$, whereas the former has none, one or two fixed points, depending on the values of a and b as will be shown below.

Another minimal chaotic mapping that has been studied is the delayed Hénon map [Sprott, 2006]. As with the Hénon map, these systems including the one in Eq. (3) typically have no direct application to particular physical systems, but they serve to exemplify the kinds of dynamical behavior, such as routes to chaos, that are common in physical chaotic systems. Thus an analytical and numerical study is warranted.

2. Fixed Points and Their Stability

In this section, we begin by studying the existence of the fixed points of the f mapping and determine their stability. The Jacobian matrix of the map (3) is

$$J(x, y) = \begin{pmatrix} b & -2ay \\ 1 & 0 \end{pmatrix},$$

and its characteristic polynomial for a fixed point (x, x) is given by

$$\lambda^2 - b\lambda + 2ax = 0. \tag{6}$$

The local stability of the two equilibria is studied by evaluating the roots of Eq. (6). Hence if $a \geq -((-b+1)/2)^2$, then the map (3) has two fixed points:

$$\begin{cases} P_1 = \left(\dfrac{b-1-\sqrt{4a-2b+b^2+1}}{2a}, \dfrac{b-1-\sqrt{4a-2b+b^2+1}}{2a} \right) \\ P_2 = \left(\dfrac{b-1+\sqrt{4a-2b+b^2+1}}{2a}, \dfrac{b-1+\sqrt{4a-2b+b^2+1}}{2a} \right), \end{cases} \tag{7}$$

whereas if $a < -((-b+1)/2)^2$, then the map (3) has no fixed point.

Thus, after some calculations, one can obtain the following results:

P_1 is unstable in the following cases:

(i) $a \geq -((-b+1)/2)^2, b < 0$.
(ii) $a \geq -((-b+1)/2)^2, a > (1/2)b + (3/4)b^2 - (1/4)$, $b > 0$.

P_1 is a saddle point in the following case:

(i) $a \geq -((-b+1)/2)^2, a < (1/2)b + (3/4)b^2 - (1/4), b > 0$.

On the other hand, P_2 is unstable in the following cases:

(i) $a \geq -((-b+1)/2)^2, a > (1/8)b^2 - (1/8)b^3 + (1/64)b^4$, $b \geq 2$.
(ii) $a \geq -((-b+1)/2)^2, a > -(1/2)b + (3/4)$, $b < 2$.
(iii) $a \geq -((-b+1)/2)^2, a \leq (1/8)b^2 - (1/8)b^3 + (1/64)b^4, b > 2$.

P_2 is stable in the following cases:

(i) $a \geq -((-b+1)/2)^2, a > (1/8)b^2 - (1/8)b^3 + (1/64)b^4, a < -(1/2)b + (3/4)$, $b < 2$.
(ii) $a \geq -((-b+1)/2)^2, a \leq (1/8)b^2 - (1/8)b^3 + (1/64)b^4, 0 \leq b \leq 2$.
(iii) $a \geq -((-b+1)/2)^2, a \leq (1/8)b^2 - (1/8)b^3 + (1/64)b^4, a > (1/2)b + (3/4)b^2 - (1/4), -2 < b < 0$.

P_2 is a saddle point in the following cases:

(i) $a \geq -((-b+1)/2)^2, a \leq (1/8)b^2 - (1/8)b^3 + (1/64)b^4, a < (1/2)b + (3/4)b^2 - (1/4), -2 \leq b < 0$.

A schematic representation of these results is given in Fig. 1, where the regions $(B_i)_{1 \leq i \leq 4}$

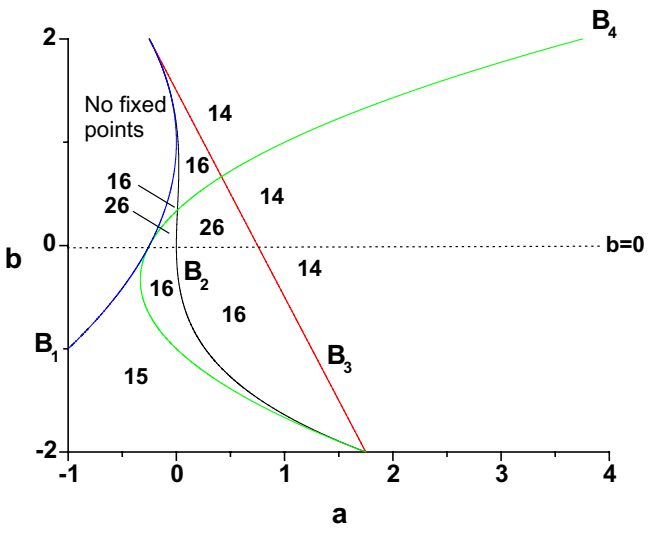

Fig. 1. Stability of the fixed points of the map (3) in the ab-plane, where the numbers on the figure are as follow: 1: P_1 is unstable, 2: P_1 is a saddle, 3: P_1 is stable, 4: P_2 is unstable, 5: P_2 is a saddle, 6: P_2 is stable, and the regions $(B_i)_{1\leq i\leq 4}$ have respectively the following boundaries: $a = -((-b+1)/2)^2$, $a = (1/8)b^2 - (1/8)b^3 + (1/64)b^4$, $a = -(1/2)b + (3/4)$, $a = (1/2)b + (3/4)b^2 - (1/4)$.

have respectively the following boundaries: $a = -((-b+1)/2)^2, a = (1/8)b^2 - (1/8)b^3 + (1/64)b^4$, $a = -(1/2)b + (3/4), a = (1/2)b + (3/4)b^2 - (1/4)$.

3. Numerical Computations

3.1. *Observation of chaotic attractors*

There are several possible ways for a discrete dynamical system to make a transition from regular behavior to chaos. Bifurcation diagrams display these routes and allow one to identify the chaotic regions in ab-space from which the chaotic attractors can be determined. In this subsection we will illustrate some observed chaotic attractors, along with some other dynamical phenomena.

For the system (3) the values of a and b that maximize the largest Lyapunov exponent with $a = 1$ and with $b = 1$ are as follow: For $a = 1$, one has $b = 0.675$ and Lyapunov exponents (base-e) of 0.171496 and 0.007595, while for $b = 1$, one has $a = 0.59948$ and Lyapunov exponents of 0.091912 and -0.074313. The corresponding chaotic attractors are shown respectively in Figs. 2(b) and 2(c) along with their basins of attraction in white. Note that the basin boundary nearly touches the attractor for these cases and is apparently a fractal for the case in Fig. 2(c).

3.2. *Route to chaos*

It is well known that the Hénon map typically undergoes a period-doubling route to chaos as the parameters are varied. By contrast, the Lozi map [Lozi, 1978] has no period-doubling route, but rather it goes directly from a border-collision bifurcation developed from a stable periodic orbit [Cao & Liu, 1998; Aziz-Alaoui *et al.*, 2001]. Similarly, the chaotic attractor given in [Elhadj, 2005] is obtained from a border-collision period-doubling bifurcation scenario. This scenario involves a sequence of pairs of bifurcations, whereby each pair consists of a border-collision bifurcation and a pitchfork bifurcation. Thus, the three chaotic systems go via different and distinguishable routes to chaos. Furthermore, the minimal quadratic chaotic attractor considered here results from a quasi-periodic route to chaos as shown in Fig. 3.

3.3. *Dynamical behaviors with parameter variation*

In this subsection, the dynamical behaviors of the map (3) are investigated numerically.

Figure 4 shows regions of unbounded (white), fixed point (gray), periodic (blue), quasi-periodic (green), and chaotic (red) solutions in the ab-plane for the map (3), where we use $|LE| < 0.0001$ as the criterion for quasi-periodic orbits with 10^6 iterations for each point. Note the agreement of Fig. 4 with the bifurcation boundaries calculated above and plotted in Fig. 1. For comparison, Fig. 5 shows a similar plot for the Hénon map [Sprott, 2003].

On the other hand, if we fix parameter $b = 0.6$ and vary $a > 0$, the map (3) exhibits the following dynamical behaviors as shown in Fig. 3: In the interval $0 < a \leq 0.45$, the map (3) converges to a fixed point. For $0.45 < a \leq 0.77$, except for a period-5 window, it converges to a quasi-periodic attractor as shown in Fig. 2(d). In the interval $0.77 < a \leq 1.07$, it converges to a chaotic attractor similar to the one in Fig. 2(b) except for a number of periodic windows. For $a > 1.07$, it does not converge.

However, if we fix parameter $a = 1$, and vary $b \geq 0$, the map (3) exhibits the following dynamical behaviors as shown in Fig. 6: For $0 < b \leq 0.099$, it converges to a fixed point. For $0.099 < b \leq 0.288$, it converges to a quasi-periodic attractor with periodic windows, and in the interval $0.288 < b \leq 0.675$, it converges to a chaotic attractor similar to the one in Fig. 2(c) except for a number of periodic and

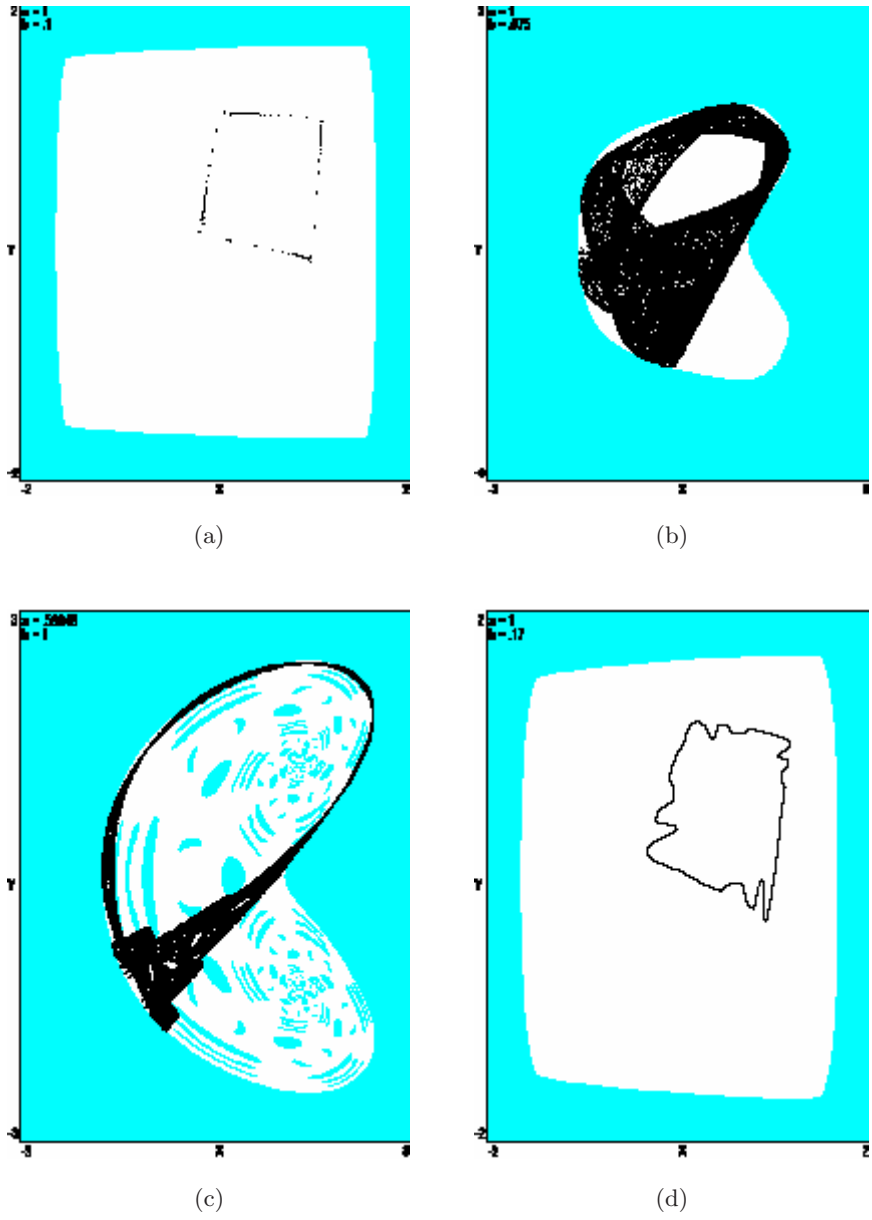

(a) (b)

(c) (d)

Fig. 2. (a) A periodic orbit of the map (3) with its basin of attraction (white) obtained for $a = 1$ and $b = 0.1$. (b) The chaotic attractor with its basin of attraction (white) for $a = 1$ and $b = 0.675$. (c) Another chaotic attractor with its basin of attraction (white) for $a = 0.59948$ and $b = 1$. (d) A quasi-periodic orbit with its basin of attraction (white) for $a = 1$ and $b = 0.17$.

quasi-periodic windows. Finally, for $b > 0.675$, the map (3) does not converge. One interesting feature is that this map is not dissipative for all combinations of a and b. In fact, there are values for which both Lyapunov exponents are positive as shown in Figs. 3(b) and 6(b), indicating hyperchaos.

Since the map (3) is not everywhere dissipative, its attractor can have a dimension equal to or even greater than 2.0 by virtue of the folding afforded by the quadratic nonlinearity. There are parameters such as $a = 0.765$ and $b = 0.854$ for which the two Lyapunov exponents are nearly equal and opposite (0.10710 and −0.10744), implying an attractor with a dimension of 1.9969 by the Kaplan–Yorke conjecture. Furthermore, when both Lyapunov exponents are positive, the dimension in principle could exceed 2.0, and this would be evident by examining the attractor in embeddings higher than 2. Takens' theorem [Takens, 1981] states that an embedding as large as $2D + 1$ might be necessary to resolve the overlaps.

As a test of this prediction, the correlation dimension was calculated for various embeddings using the extraplation method of Sprott

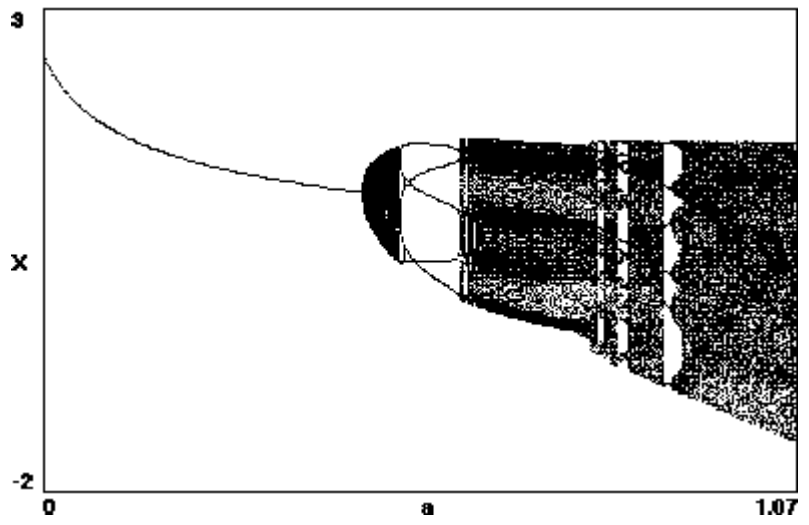

(a)

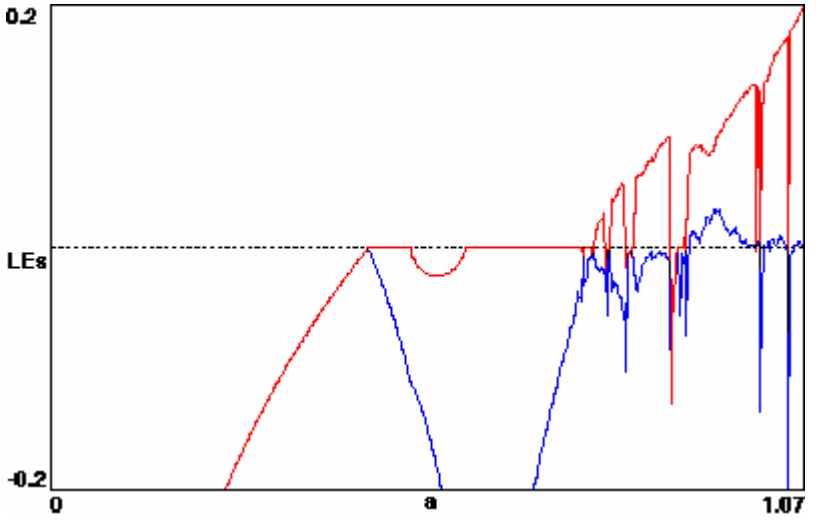

(b)

Fig. 3. (a) The quasi-periodic route to chaos for the map (3) obtained for $b = 0.6$ and $0 < a \leq 1.07$. (b) Variation of the Lyapunov exponents of map (3) versus the parameter $0 < a \leq 1.07$ with $b = 0.6$.

and Rowlands [2001], and the results are plotted in Fig. 9 for the map (3) with $a = 1$ and $b = 0.675$ where the Lyapunov exponents are 0.171496 and 0.007595. The correlation dimension is approximately constant with a value of about 1.87 for all embeddings greater than 1. Figure 10 shows the regions of the ab-plane where the system is dissipative and bounded (in black) and where it is dissipative but area-expanding (in white) as determined from the sign of the numerical average of $\log|2ay|$ over the orbit on the attractor.

These results suggest that the Takens' criterion is overly restrictive for the map (3) even though the map is noninvertible for all combinations of a and b, and hence there is not a one-to-one reconstruction for the map. On the other hand, it is well known that basin boundaries arise in dissipative dynamical systems when two or more attractors are present. In such situations each attractor has a basin of initial conditions that lead asymptotically to that attractor. The sets that separate different basins are called the basin boundaries. In some cases the basin boundaries can have very complicated fractal structure and hence pose an additional impediment to predicting long-term behavior. For the map (3) we have calculated the attractors and their basins

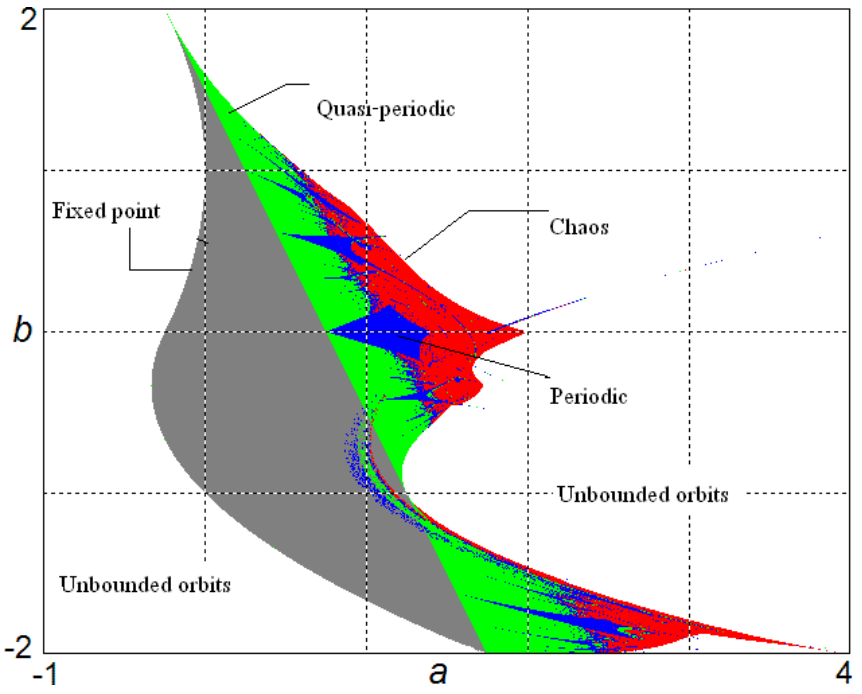

Fig. 4. Regions of dynamical behaviors in the *ab*-plane for the map (3).

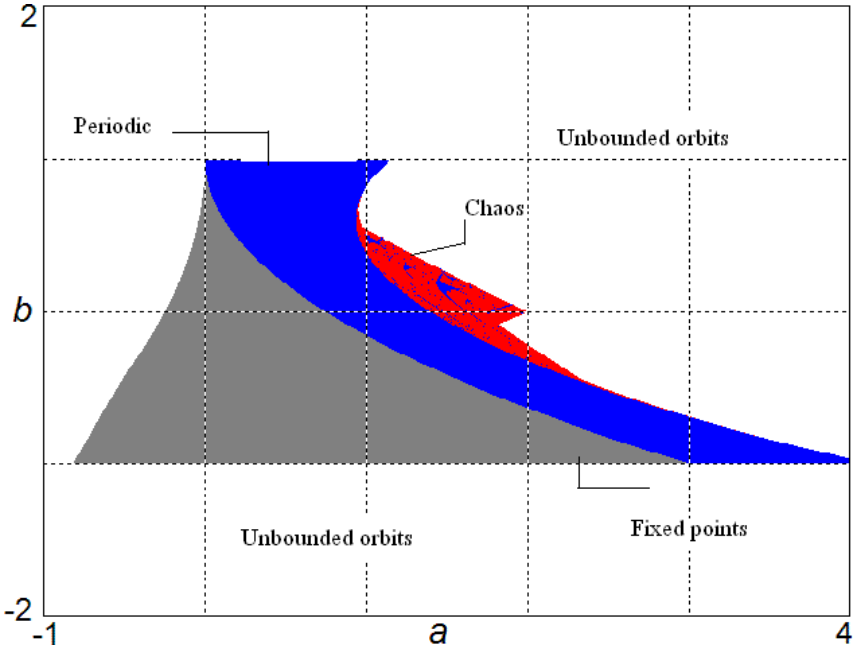

Fig. 5. Regions of dynamical behaviors in the *ab*-plane for the Hénon map [Sprott, 2003].

of attraction on a grid in *ab*-space where the system is chaotic. There is a very wide variety of possible attractors, only some of which are shown in Figs. 2, 7 and 8. Also, most of the basin boundaries are smooth, but some appear to be fractal, and this is not a result of numerical errors since the structure persists as the number of iterations of each initial condition is increased.

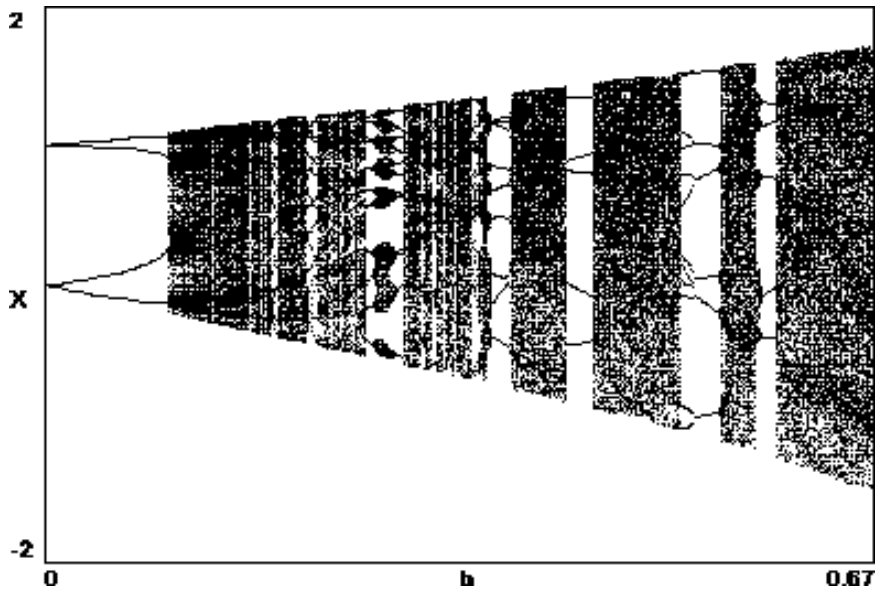

(a)

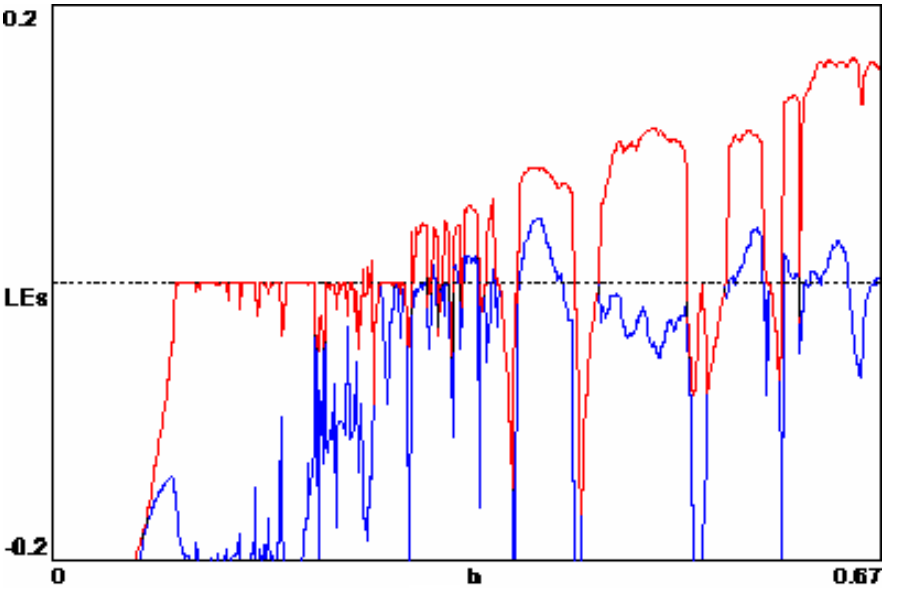

(b)

Fig. 6. (a) The bifurcation diagram for the map (3) obtained for $a = 1.0$ and $0 < b \leq 67$. (b) Variation of the Lyapunov exponents of map (3) versus the parameter $0 < b \leq 0.67$, with $a = 1$.

There are some regions in ab-space where two coexisting attractors occur as shown in the black region of Fig. 11. For example, with $a = 1$ and $b = -0.8$, a fixed point (at $x = y = 0.4329311$) coexists with a period-3 orbit, and with $a = 1$ and $b = -0.8$, fixed point (at $x = y = 0.445362$) coexists with a quasiperiodic orbit. Coexisting attractors are not evident in the chaotic region, however.

Figure 11 was obtained by using 200 different random initial conditions and looking for cases where the distribution of the average value of x on the attractor is bimodal. Since there is no rigorous test for bimodality, this was done by sorting the

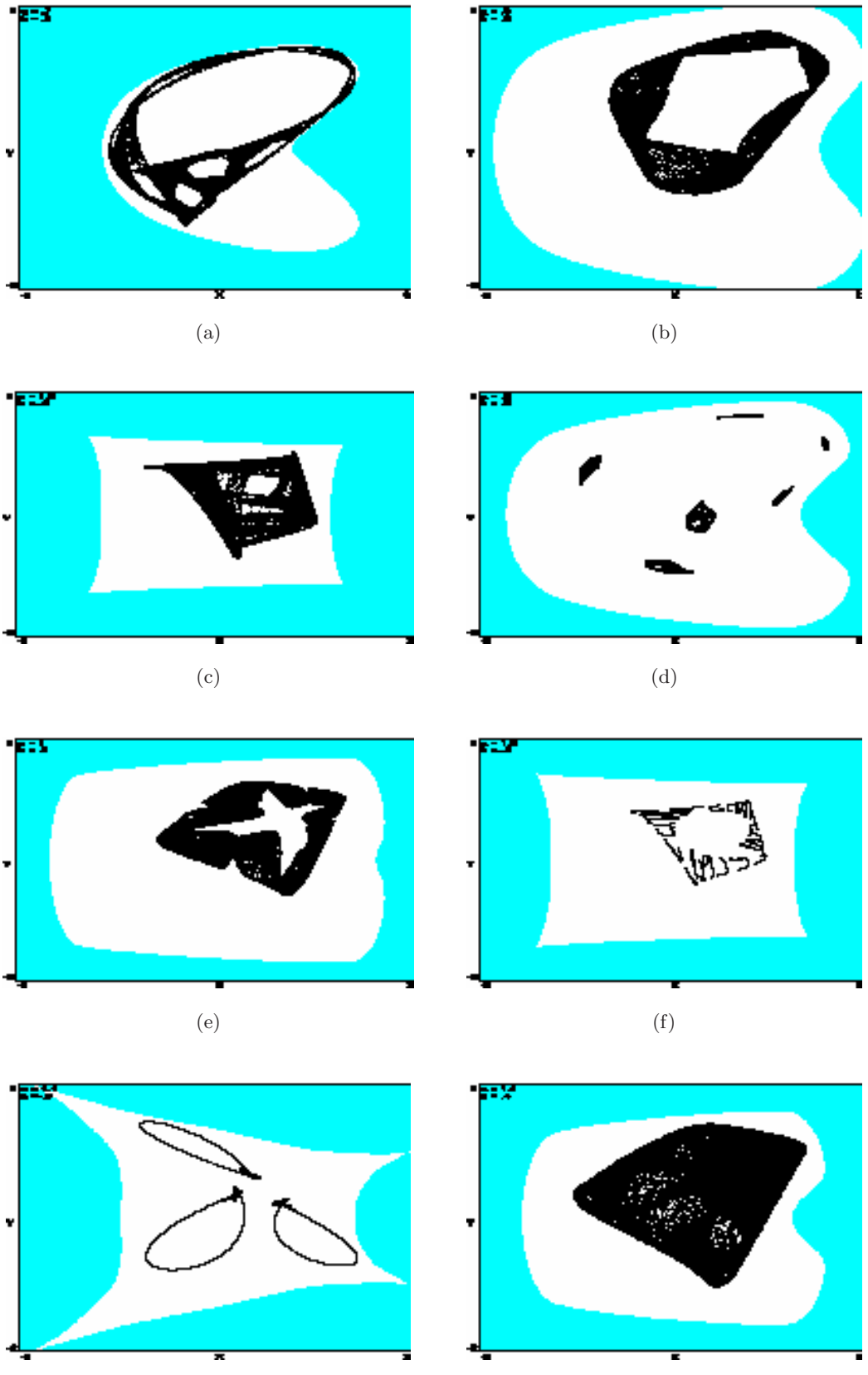

Fig. 7. Attractors for the system (3) with their basins of attraction (white) when (a) $a = 0.7, b = 0.9$, (b) $a = 0.8, b = 0.6$, (c) $a = 1.5, b = -0.2$, (d) $a = 0.9, b = 0.6$, (e) $a = 1, b = 0.3$, (f) $a = 1.3, b = -0.2$, (g) $a = 1.1, b = -0.9$, (h) $a = 1.1, b = 0.4$.

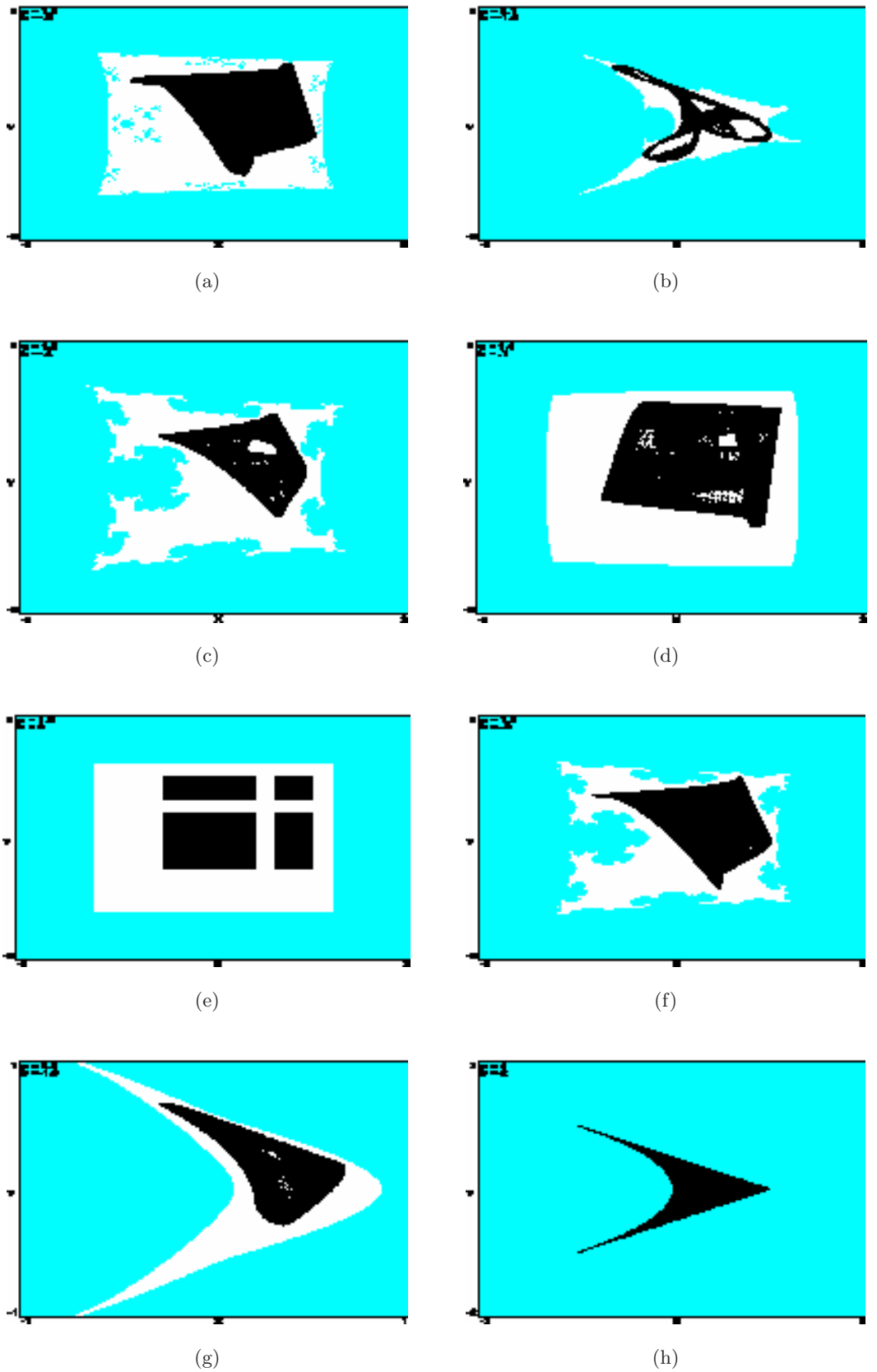

Fig. 8. Attractors for the system (3) with their basins of attraction (white) for (a) $a = 1.6, b = -0.2$, (b) $a = 2.1, b = -1.5$, (c) $a = 1.5, b = -0.4$, (d) $a = 1.4, b = 0.1$, (e) $a = 1.5, b = 0$, (f) $a = 1.6, b = -0.3$, (g) $a = 2.6, b = -1.8$, (h) $a = 4, b = -2$.

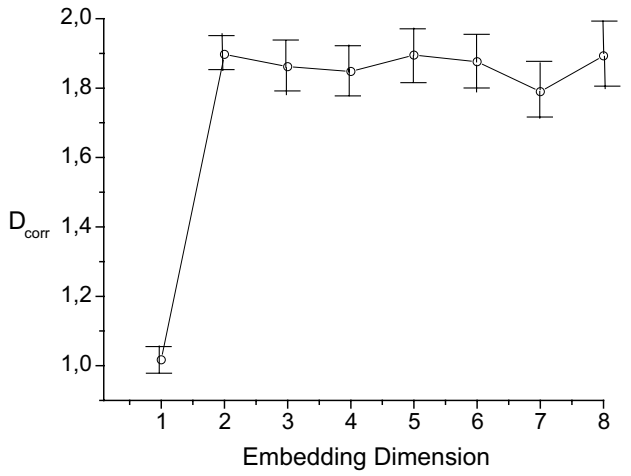

Fig. 9. Correlation dimension versus embedding dimension for the map (3) with $a = 1$ and $b = 0.675$.

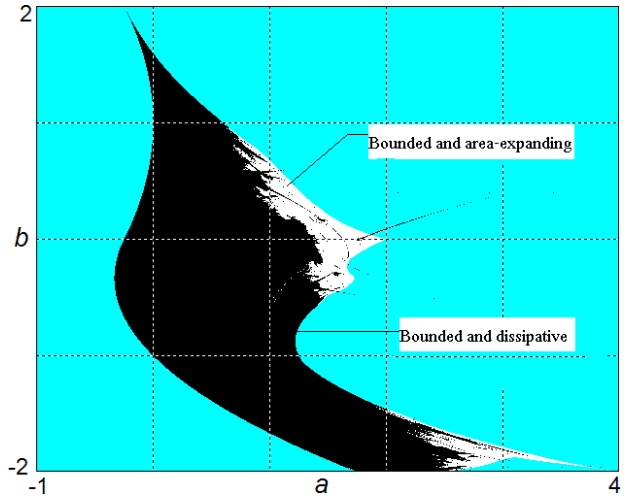

Fig. 10. The sign of the average of $\log|2ay|$ over the orbit on the attractors of the system (3) in the ab-plane defines the regions of net expansion and contraction.

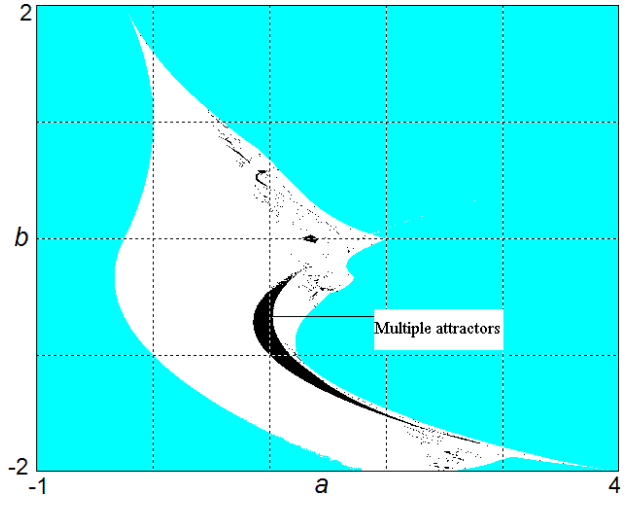

Fig. 11. The regions of ab-space for multiple attractors.

200 values of $\langle x\rangle$ and then dividing them into two equal groups. The group with the smallest range of $\langle x\rangle$ was assumed to represent one of the attractors, and a second attractor was assumed to exist if the largest gap in the values of those in the other group was twice the range of the first group. The coexisting attractors were then confirmed in a separate calculation.

4. Conclusion

We have described a minimal discrete quadratic chaotic map of the plane. Detailed dynamical behaviors of this map including fixed points, bifurcations, dynamical behavior, dimension and basin boundaries were investigated. The map is rich with interesting dynamical behavior and is thus ripe for further study.

References

Andreyev, Y. V., Belsky, Y. L., Dmitriev, A. S. & Kuminov, D. A. [1996] "Information processing using dynamical chaos: Neural networks implantation," *IEEE Trans. Neural Networks* **7**, 290–299.

Aronson, D. G., Chory, M. A., Hall, G. R. & McGehee, R. P. [1982] "Bifurcations from an invariant circle for two-parameter families of maps of the plane: A computer-assisted study," *Commun. Math. Phys.* **83**, 303–354.

Aziz-Alaoui, M. A., Robert, C. & Grebogi, C. [2001] "Dynamics of a Hénon–Lozi map," *Chaos Solit. Fract.* **12**, 2323–2341.

Benedicks, M. & Carleson, L. [1991] "The dynamics of the Hénon maps," *Ann. Math.* **133**, 1–25.

Cao, Y. & Liu, Z. [1998] "Orientation-preserving Lozi map," *Chaos Solit. Fract.* **9**, 1857–1863.

Elhadj, Z. [2005] "A new chaotic attractor from 2-D discrete mapping via border-collision period doubling scenario," *Discr. Dyn. Nature Soci.* **9**, 235–238.

Grassi, G. & Mascolo, S. [1999] "A system theory approach for designing cryptosystems based on hyperchaos," *IEEE Trans. Circuits Syst.-I: Fund. Th. Appl.* **46**, 1135–1138.

Hénon, M. [1976] "A two dimensional mapping with a strange attractor," *Commun. Math. Phys.* **50**, 69–77.

Lozi, R. [1978] "Un attracteur étrange du type attracteur de Hénon," *J. Physique. Colloque* **C5**, Supplément au n° 8, 39, 9–10.

Miller, D. A. & Grassi, G. [2001] "A discrete generalized hyperchaotic Hénon map circuit," *Circuits and Systems. MWSCAS 2001, Proc. 44th IEEE 2001 Midwest Symp.* **1**, 328–331.

Newcomb, R. W. & Sathyan, S. [1983] "An RC op amp chaos generator," *IEEE Trans. Circuits Syst.* **CAS-30**, 54–56.

Sprott, J. C. [1993] *Strange Attractors*: *Creating Patterns in Chaos* (M&T Books, NY).

Sprott, J. C. & Rowlands, G. [2001] "Improved correlation dimension calculation," *Int. J. Bifurcation and Chaos* **11**, 1865–1880.

Sprott, J. C. [2003] *Chaos and Time-Series Analysis* (Oxford University Press).

Sprott, J. C. [2006] "High-dimensional dynamics in the delayed Hénon map," *Electron. J. Theoret. Phys.* **3**, 19–35.

Takens, F. [1981] *Detecting Strange Attractors in Turbulence*, Lecture Notes in Mathematics, Vol. 898 (Springer-Verlag).